http://dx.doi.org/10.5012/bkcs.2011.32.12.4397

Computational Drug Discovery Approach Based on Nuclear Factor-κB Pathway Dynamics

Ky-Youb Nam,[†,*] Won Seok Oh,[‡] Chul Kim,[§] Miyoung Song,[§] Jong Young Joung,[‡,#] Sunyoung Kim,[‡] Jaeseong Park,[‡] Sin Moon Gang,[‡] YoungUk Cho,[#] and Kyoung Tai No[#,*]

[†]*YOUAI Co., Ltd., Suwon, Korea. [*]E-mail: kyn@youai.co.kr*
[‡]*Bioinformatics and Molecular Design Research Center, Seoul, Korea*
[§]*Korea Institute of Oriental Medicine, Daejeon, Korea*
[#]*Department of Biotechnology and Translational Research Center for Protein Function Control, Yonsei University, Seoul, Korea*
[*]*E-mail: ktno@yonsei.ac.kr*
Received July 25, 2011, Accepted October 31, 2011

The NF-κB system of transcription factors plays a crucial role in inflammatory diseases, making it an important drug target. We combined quantitative structure activity relationships for predicting the activity of new compounds and quantitative dynamic models for the NF-κB network with intracellular concentration models. GFA-MLR QSAR analysis was employed to determine the optimal QSAR equation. To validate the predictability of the IKKβ QSAR model for an external set of inhibitors, a set of ordinary differential equations and mass action kinetics were used for modeling the NF-κB dynamic system. The reaction parameters were obtained from previously reported research. In the IKKb QSAR model, good cross-validated q^2 (0.782) and conventional r^2 (0.808) values demonstrated the correlation between the descriptors and each of their activities and reliably predicted the IKKβ activities. Using a developed simulation model of the NF-κB signaling pathway, we demonstrated differences in IκB mRNA expression between normal and different inhibitory states. When the inhibition efficiency increased, inhibitor 1 (PS-1145) led to long-term oscillations. The combined computational modeling and NF-κB dynamic simulations can be used to understand the inhibition mechanisms and thereby result in the design of mechanism-based inhibitors.

Key Words : Drug design, NF-κB pathway, Inflammatory model, Quantitative structure-activity relationship, Dynamic simulation

Introduction

The NF-κB system of transcription factors plays a crucial role in inflammatory diseases. As a result, the NF-κB signaling pathway has become the most studied and best understood system of transcriptional regulation in molecular biology.[1] When upstream stimuli activate IκB kinase (IKK), IκB is phosphorylated and degraded via the ubiquitin-proteosome system.[2] IκB degradation leads to the activation of NF-κB (Fig. 1), and NF-κB signal transduction regulates various cellular responses such as inflammation, proliferation, survival, tumor promotion, metastasis, angiogenesis, cell death, and antiproliferative effects.[3]

IKKβ (IKK-2) is critical for NF-κB activation, and IKKβ inhibitors are vital for treating treat inflammatory diseases. Research has identified many IKKβ inhibitors. For example, novel quinazoline analogues were identified from the screening of an in-house diversity library.[4] From high-throughput screening of the Bayer compound library, a diarylpyridine derivative was identified as a potent IKKβ inhibitor.[5] β-carbolin analogues (Fig. 2) inhibit IKKβ with an IC_{50} of 150 nM and interfere with NF-κB activation[6,7] The thiophenecarboxamide derivative SC-514 inhibits the native IKK complex, recombinant human IKK-1/IKK-2 heterodimer, and IKKβ homodimer similarly. IKKβ inhibition by SC-514 is selective, reversible, and competitive with ATP.[8] Recently, among the 60 compounds identified as IKKβ inhibitors by a virtual screening approach, three compounds were shown to potently inhibit the IKKβ

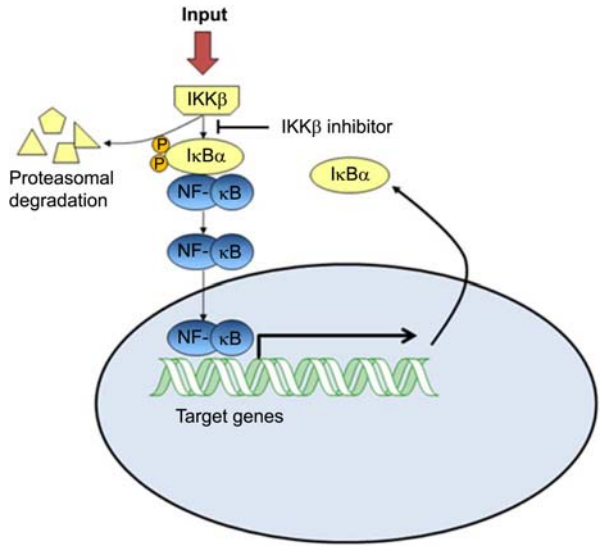

Figure 1. Schematic representation of the NF-κB signalling pathway. A pathway model for NF-κB is show with the IKK inhibitor considered.

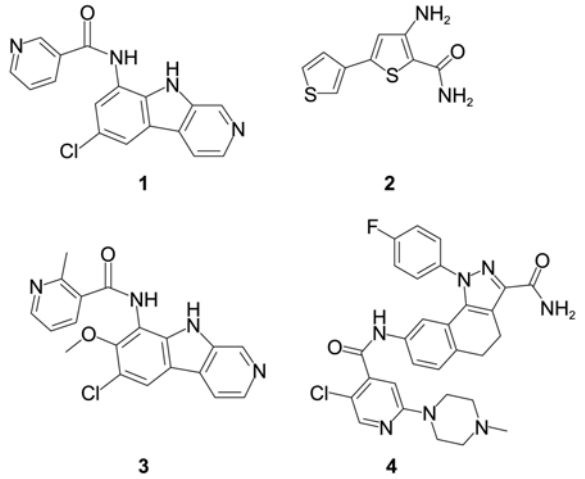

Figure 2. Four known inhibitors (PS-1145, SC-514, ML120B and PHA-408) of IKKβ.

enzyme.[9]

In this study, we suggest new computational drug discovery approach based on the cheminformatics and systems biology technique. When a compound will be predicted activity against IKKβ enzyme, quantitative concentrations of proteins in NF-κB signaling pathway will be simulated. The NF-κB signaling pathway was modeled and simulated using parameters obtained from a previous study by Hoffmann.[7] Quantitative structure activity relationships were used to predict the IKKβ activity of new compounds, and a quantitative dynamic model was applied to investigate the NF-κB network with intracellular concentration models.

Methods

QSAR Model Construction. For building a QSAR model, IKKβ inhibitor datasets were taken from BindingDB.[11,12] A subset of 93 compounds from the complete list of 132 inhibitors was utilized as a training set for QSAR modeling. The remaining 39 molecules (*ca.* 30% of the dataset) comprised an external test set for validating the QSAR model. Descriptors were calculated for each compound by employing the Topomol module in PreADMET software, which was developed by BMDRC.[13] The PreADMET program provides rapid and reliable data of drug-likeness and ADME properties. It can also calculate constitutional, electrostatic, physicochemical, geometric, and topological descriptors that have been developed in response to the need for rapid prediction of drug-likeness and ADME/toxicity data.

The Genetic function approximation-multiple linear regression (GFA-MLR) module in Discovery Studio 2.0 (DS2.0) software[14] was employed to optimize the QSAR regression equation that correlates the biological activities of IKKβ training inhibitors. The activity data of IKKβ [IC_{50}(μM)] inhibitors were converted to the logarithmic scale [$pIC_{50} = -\log IC_{50}(\mu M)$-6.0] and then used for QSAR analysis. The IKKβ QSAR model was generated with the following optimal GFA parameters: explore linear, quadratic, and spline equations at mating and mutation probabilities of 50%; population size = 500; number of genetic iterations = 30,000; and lack-of-fit (LOF) smoothness parameter = 1.0. The statistical quality of the resulting equations judged by using r^2 was the square of the correlation coefficient and represented the goodness of fit. Internal predictability of the

$$
\begin{aligned}
NF-\kappa B'(t) &= -a_4 I\kappa B\alpha(t)\bullet NF-\kappa B(t) + d_4 I\kappa B\alpha\_NF-\kappa B(t) - a_4 IKK\_I\kappa B\alpha(t)\bullet NF-\kappa B(t)\\
&\quad + d_4 IKK\_I\kappa B\alpha\_NF-\kappa B(t) + r_4 IKK\_I\kappa B\alpha\_NF-\kappa B(t) + \deg_4 I\kappa B\alpha\_NF-\kappa B(t)\\
&\quad - k_1 NF-\kappa B(t) + k_{01} NF-\kappa B_{Nuc}(t)
\end{aligned}
$$

$$
NF-\kappa B_n'(t) = k_1 NF-\kappa B(t) - a_4 I\kappa B\alpha_n(t)\bullet NF-\kappa B_n(t) + d_4 I\kappa B\alpha_n\_NF-\kappa B_n(t) - k_{01} NF-\kappa B_{Nuc}(t)
$$

$$
I\kappa B\alpha_t'(t) = tr2a + tr2k_1 NF-\kappa B_n(t)^2 - tr3 I\kappa B\alpha_t(t)
$$

$$
\begin{aligned}
I\kappa B\alpha'(t) &= -a_1 IKK(t)\bullet I\kappa B\alpha(t) + d_1 IKK\_I\kappa B\alpha(t) - a_4 I\kappa B\alpha(t)\bullet NF-\kappa B(t) + d_4 I\kappa B\alpha\_NF-\kappa B(t)\\
&\quad + tr1 I\kappa B\alpha_t(t) - \deg 1 I\kappa B\alpha(t) - tp1 I\kappa B\alpha(t) + tp2 I\kappa B\alpha_n(t)\\
I\kappa B\alpha_n'(t) &= tp1 I\kappa B\alpha(t) - tp2 I\kappa B\alpha_n(t) - a_4 I\kappa B\alpha_n(t)\bullet NF-\kappa B_n(t) + d_4 I\kappa B\alpha_n\_NF-\kappa B_n(t)
\end{aligned}
$$

$$
I\kappa B\alpha_n'(t) = tp1 I\kappa B\alpha(t) - tp2 I\kappa B\alpha_n(t) - a_4 I\kappa B\alpha_n(t)\bullet NF-\kappa B_n(t) + d_4 I\kappa B\alpha_n\_NF-\kappa B_n(t)
$$

$$
\begin{aligned}
I\kappa B\alpha\_NF-\kappa B(t) &= a_4 I\kappa B\alpha(t)\bullet NF-\kappa B(t) - d_4 I\kappa B\alpha\_NF-\kappa B(t) - a_7 IKK(t)\bullet I\kappa B\alpha(t)\bullet NF-\kappa B(t)\\
&\quad + d_1 IKK\_I\kappa B\alpha\_NF-\kappa B(t) + k_2 I\kappa B\alpha_n(t)\bullet NF-\kappa B_n(t) - \deg_4 I\kappa B\alpha\_NF-\kappa B(t)
\end{aligned}
$$

$$
I\kappa B\alpha_n\_NF-\kappa B_n'(t) = a_4 I\kappa B\alpha_n(t)\bullet NF-\kappa B_n(t) - d_4 I\kappa B\alpha_n\_NF-\kappa B_n(t) - k_2 I\kappa B\alpha_n\_NF-\kappa B_n(t)
$$

$$
\begin{aligned}
IKK'(t) &= -k_{02} IKK(t) - a_1 IKK(t)\bullet I\kappa B\alpha(t) + (d_1 + r_1) IKK\_I\kappa B\alpha(t) - a_7 IKK(t)\bullet I\kappa B\alpha(t)\bullet NF-\kappa B(t)\\
&\quad + (d_1 + r_4) IKK\_I\kappa B\alpha\_NF-\kappa B(t)\\
IKK\_I\kappa B\alpha'(t) &= a_1 IKK(t)\bullet I\kappa B\alpha(t) - (d_1 + r_1) IKK\_I\kappa B\alpha(t) - a_4 IKK\_I\kappa B\alpha(t)\bullet NF-\kappa B(t)\\
&\quad + d_4 IKK\_I\kappa B\alpha\_NF-\kappa B(t)
\end{aligned}
$$

$$
\begin{aligned}
IKK\_I\kappa B\alpha\_NF-\kappa B'(t) &= a_7 IKK(t)\bullet I\kappa B\alpha\_NF-\kappa B(t) + a_4 IKK\_I\kappa B\alpha(t)\bullet NF-\kappa B(t)\\
&\quad - (d_1 + d_4 + r_4) IKK\_I\kappa B\alpha\_NF-\kappa B(t)
\end{aligned}
$$

Figure 3. A kinetic model of NF-κB. The mathematical model of the IKKβ-IκB-NF-κB signaling module was described Hoffmann *et al.*[10]

model was characterized by the cross-validated squared correlation coefficient (q^2).

Model Construction and Simulation Protocol. The NF-κB dynamic system model was based on a set of ordinary differential equations and mass action kinetics (Fig. 3). The reaction parameters were obtained from the work of Hoffmann *et al.*[10] To investigate the effects of only IKKβ inhibitors, we did not consider the effects of IκBβ and IκBε inhibitors. The dynamic simulation model consisted of 10 ordinary differential equations describing the time evolution of NF-κB, IκBα, and IKKβ concentrations and NF-κB–IκBα, IκBα–IKKβ, and NF-κB–IκBα–IKKβ molecular complexes. The participating molecular species are assumed to translocate between two subcellular compartments: the cytoplasm and the nucleus, thus necessitating considerations about transport rates in addition to binding and reaction rates. The input into the signaling module is represented by the concentration of the active IKK. In the NF-κB dynamic simuation, all four rates are described explicitly. In general, enzymes, substrates and products of individual reactions can be shared among multiple reactions giving rise to more complex differential equations for the corresponding concentrations. Thus, in order to describe changes in the concentration of a reaction component completely, all reactions that this component participates in, plus possible transport, degradation and complex formation rates must be considered. The initial condition was 0.0 μM for free cytoplasmic IκBα and 0.1 μM for both cytoplasmic IKKβ and cytoplasmic NF-κB. All simulations were run using a simple linear ordinary differential equation (ODE) method. Treatment parameters of the linear ODE systems can be found in most standard differential equations textbooks.[15]

Results and Discussion

IKKβ QSAR Model. We employed GFA-MLR QSAR analysis to determine the optimal QSAR equation. To validate the predictability of the IKKβ QSAR model with an external set of inhibitors, we randomly selected 39 compounds and employed them as the external test set.

Eq. (1) shows the final IKKβ QSAR model. Figure 4 shows the corresponding scatter plots of experimental versus estimated biological activities of IKKβ inhibitors. Figure 4(a) is plotted the correlation of experimental and predicted activity about 93 training inhibitors, and Figure 4(b) is also plotted the correlation about 39 external test inhibitors.

$$\begin{aligned} \text{pIC50} = &-2.79826 + 1.47415^{*}\, \textit{Auto\_Geary\_02\_electronegativity} + 0.179339^{*}\, \textit{No\_NsH} \\ &- 0.087856^{*}\, \textit{SC\_06\_path} + 2.81932^{*}\, \textit{Auto\_Geary\_06\_MPEOE\_charge} \\ &+ 0.024282^{*}\, \textit{VS\_05} \end{aligned} \quad (1)$$

$$F = 60.08,\ n = 93,\ r^2 = 0.808,\ q^2 = 0.782,\ r^2_{PRESS} = 0.575$$

r^2 is the correlation coefficient of 93 training inhibitors, q^2 is the leave-one-out correlation coefficient, and r^2_{PRESS} is the predictive r^2 for the 39-compound test set. *Auto_Geary_02_electronegativity* is one of the autocorrelation descriptors with electronegativity calculated by the Geary method, which is the summation of the Pauling electronegativity difference between adjunct atoms with Geary correlations.[13] *No_NsH* is the number of single bonds between N atoms and H atoms. *SC_06_path* is a subgraph count of order 6 (path). *Auto_Geary_06_MPEOE_charge* is an autocorrelation descriptor of order 6 MPEOE charges. *VS_05* is valence shell count of order 5.[16] The IKKb QSAR model illustrates certain roles played by ligand topology in the binding process. Autocorrelation descriptors of electronegativity and MPEOE charges implied that the polar part within inhibitors forms hydrogen bonds with the hinge backbone of IKKβ. A valence shell count of order 5 means that the potential active inhibitors require a 5-membered ring for hydrophobic interaction. Good cross-validated q^2 (0.782) and conventional r^2 (0.808) values demonstrated the correlation between the descriptors and each of their activities, indicating reliable prediction of IKKβ activities.

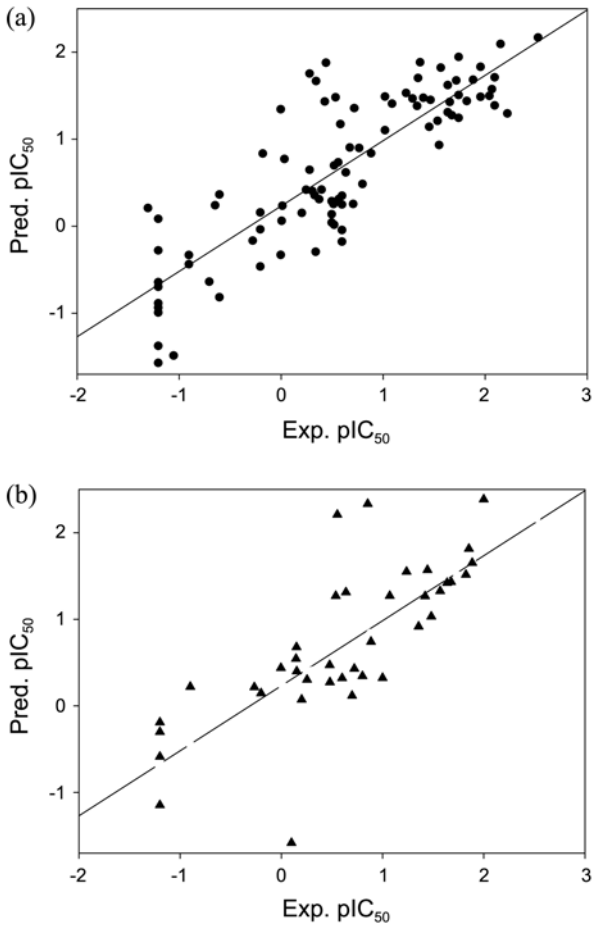

Figure 4. Experimental versus fitted and predicted activities calculated from the IKKβ QSAR model (Eq. 1). The fitted and predicted activities of training (a) and test compounds (b), respectively.

NF-κB Dynamic Simulations. We developed a simulation model of the NF-κB signaling pathway with quantitative information of reaction rates and the molecular concentrations of signaling entities. Two different inhibitors (Fig. 2)

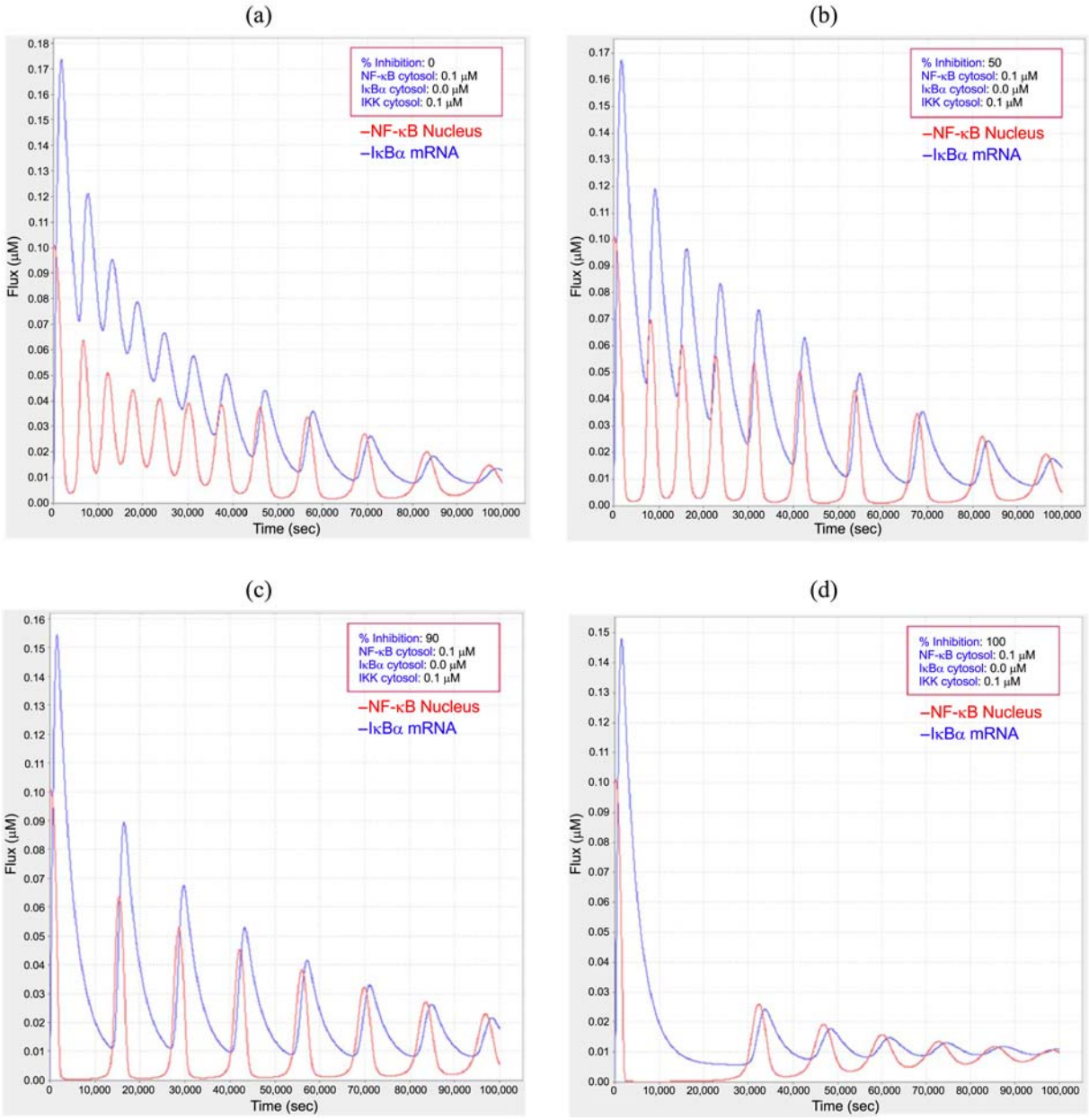

Figure 5. Computational simulation of NF-κB signalling pathway over 100,000 seconds. Oscillation of nuclear NF-κB and IκBα mRNA were simulated without inhibitor (a), with SC-514 (b), PS-1145 (c) and ideal 100% inhibitor.

were employed for the NF-κB simulation. Inhibitor 1, PS-1145, inhibits IKKβ with an IC_{50} of 150 nM.[6] The predicted IC_{50} value of the IKKβ QSAR Model was 385 nM. Inhibitor 2, SC-514, also blocks IκBα phosphorylation with an IC_{50} of ~20 μM against IKKβ.[8] The predicted IC_{50} value of the IKKβ QSAR Model was 30.57 μM. We estimated the percent inhibition of IKKβ from the IC_{50} values of the two different inhibitors, and PS-1145 was assumed to induce 90% inhibition of IKKβ because it is an extremely strong inhibitor. SC-514 showed mild inhibition, thus we assumed 50% inhibition of IKKβ as the input parameter.

Results of the normal NF-κB simulation showed that a high level of IκBα mRNA expression was achieved by increasing the time scale when compared with other inhibitor simulations. Figure 3 shows the time course of NF-κB in the cytoplasm and IκBα mRNA expression under normal and inhibitory states. The maximum level of IκBα mRNA expression exceeded 0.17 μM without inhibiting IKKβ (Fig. 5(a)); however, simulation with inhibitors showed that the maximum level of IκBα mRNA expression was slightly reduced (Fig. 5(b) and (c)). When the inhibition efficiency increased, inhibitor 1, PS-1145, led to long-term oscillations in the output (Fig. 5(c)).

To facilitate comparisons among different inhibitors of the same pathway, we calculated the area under the curve (AUC) and tabulated the efficiency of inhibitors. For PS-1145, SC-514, and complete inhibition, the differences of AUCs of IκBα mRNA expression were –3.4%, –27.9%, and

Table 1. Relative Change of AUC with various inhibitions for 100,000 seconds

Inhibitor	NF-κB in Nucleus	IκB mRNA expression
No inhibition (0%)	100.0	100.0
SC-514 (50%)	82.1	96.6
PS-1145 (90%)	62.6	72.1
Ideal (100%)	46.3	42.8

Table 2. Relative Change of AUC with various inhibitions for 5400 seconds

Inhibitior	NF-κB in Nucleus	IκBα incytosol
No inhibition (0%)	100.0	100.0
SC-514 (50%)	89.6	107.4
PS-1145 (90%)	77.2	127.9
Ideal (100%)	71.9	144.1

−57.2%, respectively, based on the simulations reported in Table 1. The experimental percent inhibition showed similar results, which indicated that PS-1145 elicited 20-50% inhibition of cell line proliferation after 48-hour incubation with PS-1145.[7] For 5400 seconds simulations, we analyzed the relative change of AUC about NF-κB in nucleus and IκBα in cytoplasm. The AUC of NF-κB in nucleus quantitatively decreased −10.4%, −22.8% and −29.1%, and AUC of IκBα in cytoplasm increased 7.4%, 27.9% and 44.1% in Table 2. These results qualitatively consisted with the results that Multiple Myeloma cells were pre-treated with 0.125-40 μM PS-1145 for 90 min.[7]

We examined the effect of the IKKβ inhibitor (ML120B) on NF-κB nuclear translocation and DNA binding activity. ML120B, inhibitor 3 in Figure 2, was employed for the NF-κB simulation for 10 hours. ML120B, inhibits IKKβ with an IC_{50} of 60 nM.[17] The predicted IC_{50} value of the IKKβ QSAR Model was 534.4 nM. From Dwn D. *et al.* work, [17] we could assumed the Hillslope of −1.7008 in Eq. (2). The Hillslope characterizes the slope of the curve at its midpoint. This is a typical dose-response curve with a variable slope parameter. Where mM is a fixed inhibitor concentration. IC_{50} can be fit to the data using SigmaPlot (Version 11, Systat Software, Inc.)[18]

$$\%Inhibition = \min\% + \frac{\max\% - \min\%}{1 + (\mu M/IC_{50})^{Hillslope}} \quad (2)$$

We applied the Hillsolpe and IC_{50} from QSAR predictions to the dose-dependent inhibition of IKKβ inhibitors (ML120B and PHA-408) in Figure 6(a). ML120B blocked nuclear translocation of NF-κB with an IC_{50} of 2.4 μM.[17] We simulated the relative change of % Inhibtion about NF-κB in nucleus in Figure 6(b). ML120B inhibited nuclear translocation of NF-κB with an IC_{50} of 0.95 μM by NF-κB dynamics simulations. PHA-408 inhibits IKKβ with an IC_{50} of 40 nM.[18] The predicted IC_{50} value of the IKKβ QSAR Model was 6.9 nM. PHA-408 is a selective and potent inhibitor than ML120B. Mbalaviele, B. *et al.*[19] shows the

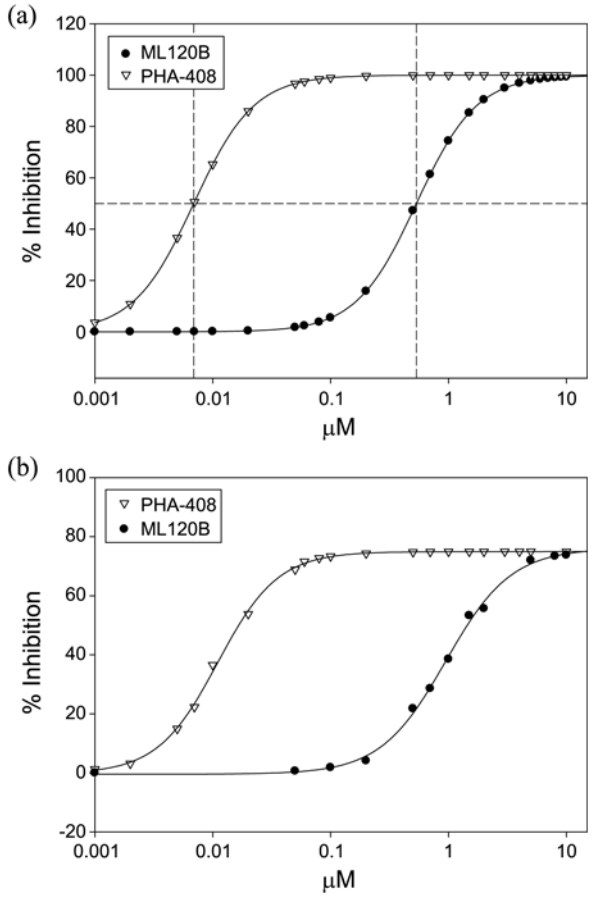

Figure 6. ML120B and PHA-408 are a potent and selective inhibitor of IKKβ. (a), dose-dependent inhibition of IKK complex, (b) two inhibitors inhibit NF-κB cytoplasm to nuclear translocation.

Table 3. Inhibitory activity of ML120B and PHA-408 in IKKβ and NF-κB in Nucleus

μM	IKKβ (*%Inhibition*)		NF-κB in Nucleus (*%Inhibition*)	
	ML120B	PHA-408	ML120B	PHA-408
0.001	0.00	3.61	0.00	0.03
0.005	-	36.64	-	14.95
0.01	-	65.27	-	36.50
0.02	-	85.94	-	53.78
0.05	0.63	96.67	0.63	68.87
0.1	1.79	98.95	1.79	73.31
0.2	4.11	99.68	4.11	74.31
0.5	21.76	99.93	21.76	74.79
0.7	28.54	99.96	28.54	74.86
1	38.51	99.99	38.51	74.91
1.5	53.29	99.99	53.29	74.93
2	55.64	99.99	55.64	74.93
5	71.97	100.00	71.97	74.96
8	73.38	100.00	73.38	74.96
10	73.78	100.00	73.78	74.96

PHA-408 quantitatively inhibited the NF-κB phosphorylation and DNA binding activity. PHA-408 blocked NF-κB phosphorylation with an IC_{50} of 30-40 nM. PHA-408 inhibited

nuclear translocation of NF-κB with an IC_{50} of 11.0 nM by NF-κB dynamics simulations. Table 3 tabulated the inhibitory activity of ML120B and PHA-408 in IKKβ and NF-κB in Nucleus. Both ML120B and PHA-408 completely blocked IκB and NF-κB phosphorylation. We used NF-κB dynamic simulation to predict and quantify nuclear translocation of NF-κB in the absence or presence of ML120B and PHA-408. Our results of NF-κB dynamic simulation are consistent with experimental data, respectively.[17,19] PHA-408 shows experimental 68.6-fold and theoretically 87.3-fold stronger activity than ML120B in nuclear translocation of NF-κB. From this study, we proposed that the combined QSAR model for predicting compound activity and dynamics simulation of the NF-κB signaling pathway will provide new insights in inflammation therapy.

Conclusions

Significant progress has been made in recent years regarding the NF-κB signal transduction pathway and the role of NF-κB in inflammation, proliferation, survival, tumor promotion, metastasis, angiogenesis, cell death, and antiproliferative effects. IKKβ is critical for NF-κB activation, thus IKKβ is a potential therapeutic target for NF-κB–related diseases. In this work, we investigated a computational modeling technique (QSAR) and dynamic simulations of the NF-κB signaling pathway in the presence or absence of inhibitors. The IKKb QSAR model was successfully built and was shown to predict the efficacy of inhibitors. Dynamic simulations of the NF-κB signaling pathway could be used to analyze the effects of inhibitors on IκBα mRNA expression and NF-κB translocation. Therefore, we propose that the combined computational modeling and dynamic simulations could help to understand the inhibition mechanisms and thereby result in the design of mechanism-based inhibitors.

Acknowledgments. This work was supported by "Development of whole lifetime preventive management system for hypertension" project of KIOM (K11201), and Ministry for Health, Welfare & Family Affairs (A101836-1011-0000600), Republic of Korea.

Supplementary Data. Supplementary data associated with this article can be found in the online version.

References

1. Karin, M. *Nat. Rev. Drug Discov.* **2004**, *3*, 17-26.
2. Liou, H. C. *J. Biochem. Mol. Biol.* **2002**, *34*, 537-546.
3. Baud, V.; Karin, M. *Nat. Rev. Drug Discov.* **2009**, *8*, 33-40.
4. Palanki, M. S. S.; Gayo-Fung, L. M.; Shevlin, G. I.; Erdman, P.; Sato, M.; Goldman, M.; Ransone, L. J.; Spooner, C. *Bioorg. Med. Chem. Lett.* **2002**, *12*, 2573-2577.
5. Murata, T.; Shimada, M.; Sakakibara, S.; Yoshino, T.; Kadono, H.; Masuda, T.; Shimzaki, M.; Shintani, T.; Fuchikami, K.; Sakai, K.; Inbe, H.; Takeshita, K.; Niki, T.; Umeda, M.; Bacon, K. B.; Ziegelbauer, K. B.; Lowinger, T. B. *Bioorg. Med. Chem. Lett.* **2003**, *13*, 913-918.
6. Castro, A. C.; Dang, L. C.; Siucy, F.; Grenier, L.; Mazdiyasni, H.; Hottelet, M.; Parent, L.; Pien, C.; Palombella, V.; Adams, J. Bioorg. *Med. Chem. Lett.* **2003,** *13*, 2419-2422.
7. Hideshima, T.; Chauhan, D.; Richardson, P.; Mitsiades, C.; Mitsides, N.; Hayashi, T.; Munshi, N.; Dang, L.; Castro, A.; Palombella, V.; Adams, J.; Anderson, K. C. *J. Biol. Chem.* **2002,** *277*, 16639-16647.
8. Kishore, N.; Sommers, C.; Mathialagan, S.; Guzova, J.; Yao, M.; Hauser, S.; Huynh, K.; Bonar, S.; Mielke, C.; Albee, L.; Weier, R.; Graneto, M.; Hanau, C.; Perry, T.; Tripp, C. S. *J. Biol. Chem.* **2003**, *278*, 32861-32871.
9. Nagarajan, S.; Choo, H.; Cho, Y. S.; Oh, K.-S.; Lee, B. H.; Shin, K. J.; Pae, A. N. *Bioorg. Med. Chem.* **2010**, *18*, 3951-3960.
10. Hoffmann, A.; Levchenko, A.; Scott, M. L.; Baltimore, D. *Science* **2002**, *298*, 1241-1245.
11. Chen, X.; Lin, Y.; Liu, M.; Gilson, M. K. *Bioinformatics* **2002**, *18*, 130-139.
12. Liu, T.; Lin, Y.; Wen, X.; Jorissen, R. N.; Gilson, M. K. *Nucleic Acids Res.* **2007**, *35*, D198-201.
13. PreADMET, *version 2.0*, 2008, Bioinformatics and Molecular Design Research Center, Seoul, Korea, Freely Available from: http://preadmet.bmdrc.org.
14. Discovery Studio, *Version 2.1*, 2007, Accelrys, Inc., San Diego, Calif.
15. Edelstein-Keshet, L. *Mathematical Models in Biology*, McGraw Hill: New York, 1988; p 218.
16. Randic, M. *J. Chem. Inf. Comp. Sci.* **2001**, *41*, 627-630.
17. Wen, D.; Nong, Y.; Morgan, J. G.; Ganurde, P.; Bielecki, A.; DaSilva, J.; Keaveney, M.; Cheng, H.; Fraser, C.; Schopf, L.; Hepperle, M.; Hearriman, G.; Jaffee, B. D.; Ocain, T. D., Xu, Y. *J. Pharmacol. Exp. Ther.* **2006**, *317*, 989-1001.
18. SigmaPlot, *Version 11.0*, 2008, Systat Software, Inc. San Jose, USA
19. Mbalaviele, G.; Sommers, C. D.; Bonar, S. L.; Mathialagan, S.; Schindler, J. F.; Guzova, J. A.; Shaffer, A. F.; Melton, M. A.; Christine, L. J.; Tripp, C. S.; Chiang, P.-C.; Thompson, D. C.; Hu, Y.; Kishore N. *J. Pharmacol. Exp. Ther.* **2009**, *329*, 14-25.